

Nanoscale

Accepted Manuscript



This is an *Accepted Manuscript*, which has been through the Royal Society of Chemistry peer review process and has been accepted for publication.

Accepted Manuscripts are published online shortly after acceptance, before technical editing, formatting and proof reading. Using this free service, authors can make their results available to the community, in citable form, before we publish the edited article. We will replace this *Accepted Manuscript* with the edited and formatted *Advance Article* as soon as it is available.

You can find more information about *Accepted Manuscripts* in the [Information for Authors](#).

Please note that technical editing may introduce minor changes to the text and/or graphics, which may alter content. The journal's standard [Terms & Conditions](#) and the [Ethical guidelines](#) still apply. In no event shall the Royal Society of Chemistry be held responsible for any errors or omissions in this *Accepted Manuscript* or any consequences arising from the use of any information it contains.

SCHOLARONE™
Manuscripts

Nanoscale Accepted Manuscript

ARTICLE

A Facile Method for Synthesis of Quaternary Ag-In-Zn-S Alloyed Nanorods

Cite this: DOI: 10.1039/x0xx00000x

Xiaosheng Tang^{a*}, Zhigang Zang^{a*}, Zhiqiang Zu^a, Weiwei Chen^a, Yan Liu^a, Genquan Han^a, Xiaohua Lei^a, Xianmin Liu^a, Xiaoqin Du^a, Weimin Chen^a, Yu Wang^b, Junmin Xue^c

Received 00th January 2012,
Accepted 00th January 2012

DOI: 10.1039/x0xx00000x

www.rsc.org/

Ag-In-Zn-S nanorods with tunable photoluminescence were synthesized by a facile approach. And the as-prepared Ag-In-Zn-S nanorods demonstrated a long fluorescence lifetime achieved to 1.248 μ s. Moreover, Ag-In-Zn-S nanorods with nail shape and rod-particle dimer structures were successfully prepared by adjusting reaction parameters.

Introduction

Semiconductor nanocrystals have attracted considerable attention because of their unique electronic and optical properties, allowing their use in the development of light-emitting diodes (LEDs)¹⁻⁴, solar cell materials and biolabels⁵⁻⁷. In recent decades, II-VI semiconductor nanoparticles have already been extensively studied for fluorescent labeling in biological research for their excellent optical property⁸⁻¹⁰. However, a large number of conventional II-VI semiconductor nanoparticles contain toxic environmental unfriendly elements such as Hg, Cd and Pb, which limited their further applications¹¹⁻¹⁵. Therefore, it is a challenge to develop alternative luminescent semiconductor nanocrystals that do not contain any toxic heavy metal ions. Ternary I-III-VI₂ semiconductor materials, such as AgInS₂¹⁶⁻²², CuInS₂^{14, 23-25}, AgGaS₂²⁶ and Cu(In_xGa_{1-x})S₂^{27, 28}, have been widely investigated for their potential applications in photovoltaic solar cells, light emitting diodes, non-linear optical devices, and photocatalytic H₂ evolution under visible light irradiation. Recently, several approaches have been employed to prepare I-III-VI₂ nanocrystals using solvothermal methods, decomposition of single-source methods, and hot injection techniques¹⁶⁻²². In our former research, hot injection method was successfully used for synthesis of CuInS₂-ZnS and AgInS₂-ZnS alloy nanoparticles with bright and tunable photoluminescence^{29, 30}. However, most of the research was focused on the synthesis of

nanoparticles, while the corresponding crystallographic growth mechanism was not fully studied.

The bandgap of semiconductor nanoparticles could be adjusted by varying the size based on the quantum confinement effect and the chemical composition^{11, 28}. Moreover, the shape of nanoparticles could also influence the photoluminescence^{28, 31-34}. For instance, it was reported that nanorods and nanowires were observed to have different optical properties from those of nanoparticles³¹⁻³⁴. Therefore, it is still a challenge for developing a simple method to tune the shape of semiconductor nanoparticles. Despite the efforts mentioned above to synthesize AgInS₂ nanocrystals for strong photoluminescence, more studies are required to develop a facile synthesis method for the preparation of color-tunable Ag-In-Zn-S nanorods.

Herein, we demonstrate a facile solution based route to synthesize Ag-In-Zn-S nanorods with tunable emissions. In this method, Ag-In-Zn-S nanorods with different aspect ratios were obtained by changing the composition of the precursors. The emission color of the resulting Ag-In-Zn-S nanorod was tuned by adjusting the amount of Zn. The obtained Ag-In-Zn-S nanorods showed adjustable photoluminescence spectra from 550 nm to 650 nm. Furthermore, the as-prepared Ag-In-Zn-S nanorods possess lifetimes much longer than that of Ag-In-Zn-S nanoparticles, which could avoid the

disturbance of autofluorescence of biological tissues and imply its potential application in the time resolved fluoroimmunoassay.

Experimental

Materials. Silver nitrate (AgNO_3 , $\geq 98\%$), silver acetate (AgAc , $\geq 98\%$), oleic acid (99.0%), zinc acetate ($\text{Zn}(\text{Ac})_2$, $\geq 90\%$), trioctylphosphine (TOP, 90%), technical grade 1-octadecene (ODE, 90%), indium(III) acetate ($\text{In}(\text{Ac})_3$, 99.99%), oleylamine (OA, 70%), 1-dodecanethiol (DDT, $\geq 98\%$), sulfur (S, 90%) and technical grade zinc stearate were purchased from Sigma-Aldrich. Toluene (99.99%), ethanol (99.9%) and chloroform (99.99%) were purchased from Fisher Scientific. All the chemicals were used as received.

The preparation of Ag-In-Zn-S nanorods

1, Synthesize of Ag-In-Zn-S nanorods

0.1 mM AgAc , 0.1 mM $\text{In}(\text{Ac})_3$, 0.1 mM $\text{Zn}(\text{Ac})_2$, 5 mM (1.2 mL) 1-dodecylthiol, 0.2 mM (40.7 mg) oleic acid and 4 mL of ODE in a 100 mL three-necked bottle were ultrasonicated for 5 mins. The reaction mixture was heated to the temperature of 180°C under a nitrogen atmosphere with magnetic stirring. The reaction was kept for 30 mins; 0.3 mM sulfur dissolved in oleylamine at 180°C was injected into it. Subsequently, the temperature increased to 210°C reacted for different time. The obtained nanorods were first washed using absolute ethanol and toluene so as to remove unreacted precursors, and the washing process was repeated three times. The purified nanorods were then dispersed in toluene or chloroform for storage.

2, Synthesize of Ag-In-Zn-S nanorods and dimer structure

0.1 mM AgAc , 0.1 mM $\text{In}(\text{Ac})_3$, 0.1 mM $\text{Zn}(\text{Ac})_2$, 5 mM (1.2 mL) 1-dodecylthiol, 3 mM (610.5 mg) oleic acid and 4 mL of ODE in a 100 mL three-necked bottle were sonicated for 30 mins. The reaction mixture was heated to the temperature of 180°C under a nitrogen atmosphere with magnetic stirring. The reaction was kept for 30 mins; 0.3 mM sulfur dissolved in oleylamine at 180°C was injected into it. Subsequently, the temperature was increased to 210°C for reaction with different time. The obtained nanorods were first washed using absolute ethanol and toluene so as to remove unreacted precursors, and the washing process was repeated three times. The purified nanorods were then dispersed in toluene or chloroform for storage.

3, One pot synthesis of Ag-In-Zn-S nail-like nanorods

Ag-In-Zn-S nail-like nanorods were prepared by thermal decomposition of a mixture of 0.1 mM AgNO_3 , 0.1 mM $\text{In}(\text{Ac})_3$ and 5 mM (1.2 mL) 1-dodecylthiol in a 100 mL three-necked bottle with 4 mL of ODE, 0.2 mM (56.4 mg) oleic acid, and about $46.5\ \mu\text{L}$ of TOP. The reaction mixture was heated to the temperature of 60°C under a nitrogen atmosphere with magnetic stirring. The reaction was kept for 60 mins, 0.1 mM zinc stearate dissolved in oleylamine and ODE (oleylamine/ ODE=4/1) at 120°C , and 0.3 mM sulfur powder was dissolved in oleylamine and ODE (oleylamine/ODE = 4/1) at 120°C . 10 drops of sulfur solution were added in the reaction three-necked bottle and 10 drops of zinc stearate solution was added subsequently, keep reaction for 5mins, and repeating added zinc stearate and sulfur solution till all chemicals were added. Then the temperature was increased to 210°C and keep reaction for 2 hrs. The obtained nanorods were first washed using absolute ethanol and toluene so as to remove unreacted precursors, and the washing process was repeated three times. The purified nanorods were then

dispersed in toluene or chloroform for storage.

Characterizations

X-ray diffractometry (XRD) was carried out using an Advanced Diffractometer System (D8 Advanced Diffractometer System, Bruker, Karlsruhe, Germany). All transmission electron microscopy (TEM) images were obtained using JEOL 3010 microscope at an acceleration voltage of 200 kV. Samples were prepared by dipping carbon-coated copper grids into the sample solution followed by drying at room temperature. Photoluminescence (PL) spectra were measured in open-sized 1 cm path-length quartz by using Perkin Elmer LS 55 spectrofluorimeter.

Results and discussion

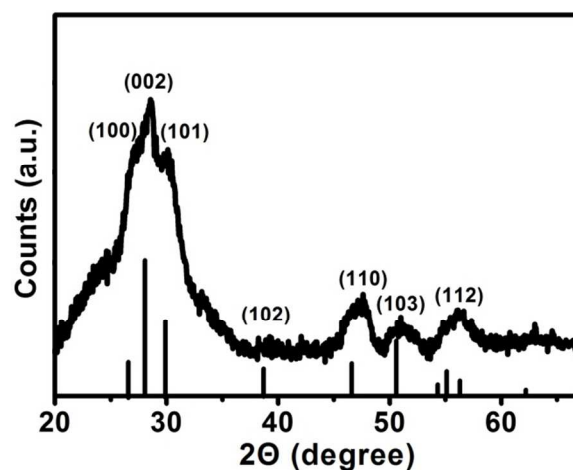


Figure 1. XRD pattern of the Ag-In-Zn-S straight nanorods.

Typical Ag-In-Zn-S nanorods were prepared via thermolysis of the mixture of silver acetate, indium acetate, zinc acetate and *n*-dodecylthiol in ODE solution at 180°C . Surfactants such as TOP and oleic acid were added as the protecting ligands. Sulphur powder was dissolved in oleylamine, and was injected into the reaction. Figure 1 presents the XRD pattern of the Ag-In-Zn-S straight nanorods collected. From the XRD peaks positioned at 2θ of 28.4° , 47.6° and 56.1° were observed, which corresponds with the (002), (110) and (112) indices, respectively, of hexagonal $\text{InAgZn}_2\text{S}_4$ crystal structure (JCPDF 25-0383)^{16, 30}. Other characteristic peaks of hexagonal were also could be found in the XRD pattern of Ag-In-Zn-S nanorods which were marked in Figure 1. For confirming the elements composition of the as-synthesized sample, energy dispersive X-ray spectroscopy was used for testing. As shown in S_Figure 1, four signals from silver, indium, zinc and sulphur elements were found in the spectrum, which demonstrated the sample was comprised of Ag, In, Zn and S.

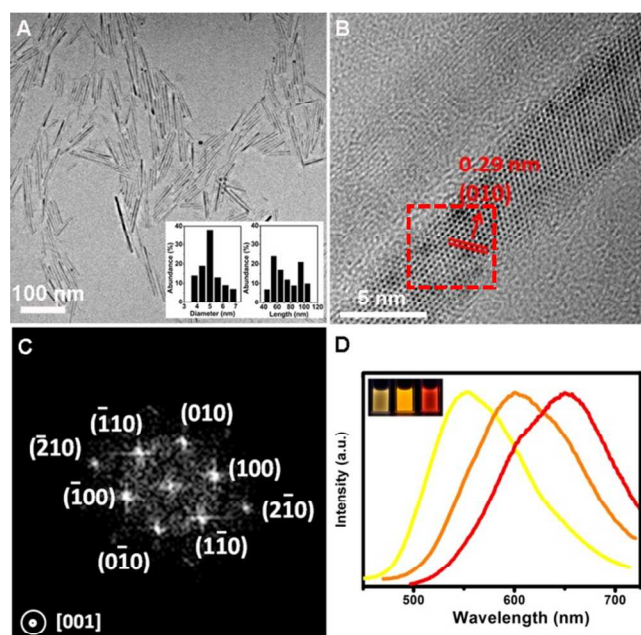
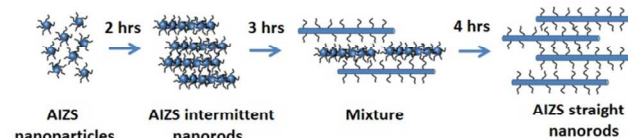


Figure 2. (A) TEM images of the Ag-In-Zn-S straight nanorods (inset: histograms showing the diameter and length distribution of the nanorods) (B) HRTEM image of one typical straight nanorod, (C) is the 2D-FFT images of the as-synthesized nail-like nanorods of the different areas of Figure 2B labeled red square. (D) PL spectra of Ag-In-Zn-S nanorods with different emissions (inset: Photography pictures of the Ag-In-Zn-S nanorods with different emissions dispersed in toluene under excitation of 365 nm.).

The morphology of the Ag-In-Zn-S samples was measured by TEM technique. From the TEM image of Figure 2A, it can be seen that high quality Ag-In-Zn-S nanorods were obtained. The as-synthesized Ag-In-Zn-S nanorods possessed a narrow size distribution, with an average width of ~ 5 nm, and length ranging from 60 to 100 nm. Figure 2B shows the HRTEM image of part of a single Ag-In-Zn-S nanorod. The lattice of the single Ag-In-Zn-S nanorod could clearly be observed, which indicated the high quality crystalline of Ag-In-Zn-S nanorods structure. Additionally, the two-dimensional fast Fourier transform (2D-FFT) of the relevant images was introduced (Figure 2C). As shown in Figure 2C, the distance between two adjacent planes in the labelled is measured to be 0.29 nm, corresponding to (010) planes of hexagonal structured, which is also consistent with the results obtained from XRD patterns^{34, 35}. The optical behaviors of the obtained Ag-In-Zn-S nanorods were characterized. Figure 2D presents the PL properties of Ag-In-Zn-S nanorods with different emission under excitation of UV (365 nm). The emission peaks wavelength were centered at 550 nm, 602 nm and 650 nm of nanorods and their corresponding photoluminescence quantum yields were 38%, 42% and 44% (S Figure 2). The emission peaks wavelength were centered at 550 nm, 602 nm and 650 nm of nanorods, the tunable photoluminescence spectra were adjusted by the ratios of Zinc (S Table 1), which has been verified in the AgInS-ZnS alloy nanoparticles system²⁹. The corresponding photography pictures of the Ag-In-Zn-S nanorods with different emissions under excitation of 365 nm was shown in Figure 2D (inset), the

colors of the Ag-In-Zn-S nanorods were tuned from yellow to red.



Scheme 1. Schematic illustration showing the growth of Ag-In-Zn-S nanorods.

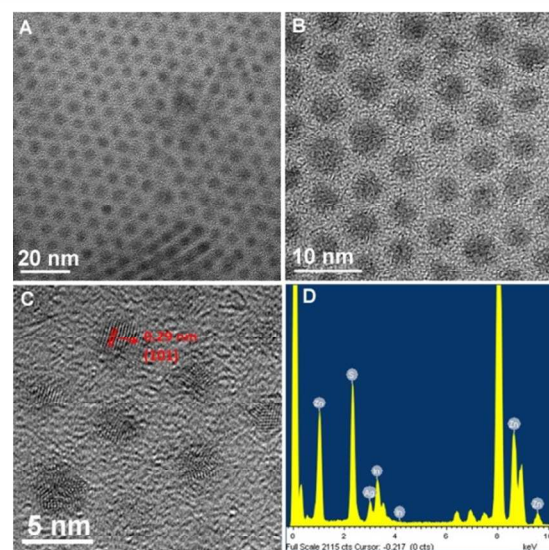


Figure 3. (A) TEM images of the Ag-In-Zn-S nanoparticles, (B) Higher magnified TEM image of nanoparticles. (C) Higher resolution TEM image of nanoparticles. (D) EDX spectra of the Ag-In-Zn-S nanoparticles.

In order to further study the detailed formation mechanism of Ag-In-Zn-S nanorods, further analysis was performed. The proposed schematic illustration of the growth of Ag-In-Zn-S nanorods was shown in Scheme 1. Figure 3A shows the samples prepared for 5 mins. It could be observed that the size of the Ag-In-Zn-S nanoparticles was ~ 4 nm and the size distribution was quite narrow. A higher magnified TEM image was shown in Figure 3B, the nanoparticles were distributed in hexagonal order. The HRTEM shown in Figure 3C further confirmed the structure of the as-obtained nanoparticles. It can be seen the lattice distance of the as-obtained nanoparticles was 0.29 nm, which is consistent with the (010) planes of Ag-In-Zn-S^{34, 35}. The EDX spectrum shown in Figure 3D indicated the compositions of the as-obtained nanoparticles were Ag, In, Zn and S elements, which is consistent with the S Figure 1. A similar system of Cu-Zn-In-S spherical nanoparticles with size about 3 nm could be achieved by a sample method. However, they did not obtain Cu-Zn-In-S rods⁴. In our developed process, more oleic acid was introduced in this reaction, which would result in the rod structure.

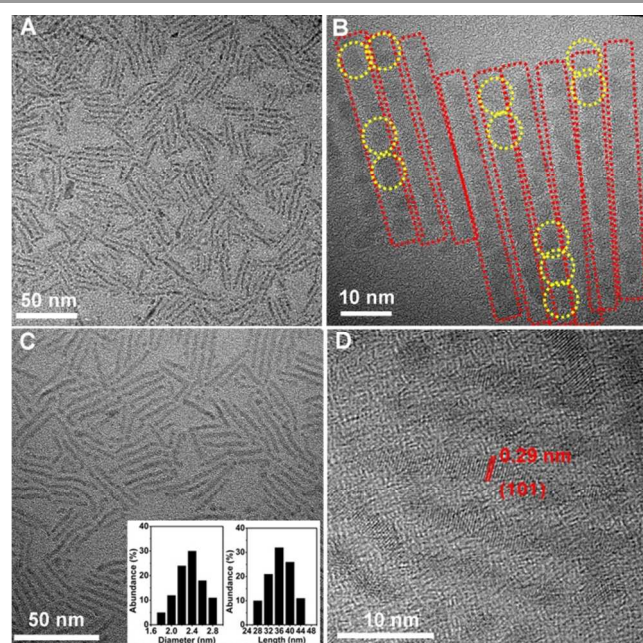


Figure 4. (A) TEM image of the Ag-In-Zn-S intermittent nanorods reaction for 2 hrs. (B) High resolution TEM image of Ag-In-Zn-S nanorods (C) TEM image of the Ag-In-Zn-S nanorods (inset: histograms showing the diameter and length distribution of the nanorods) (D) HRTEM image of several typical nanorods,

After reaction for 2 hrs, Ag-In-Zn-S intermittent nanorods were obtained. Figure 4A was the TEM image of the Ag-In-Zn-S intermittent nanorods. It was observed that the Ag-In-Zn-S nanorods retained the rod shape, but the rod structure was not fully straight. Under more careful observation, the Ag-In-Zn-S intermittent nanorods were formed by several nanoparticles which were arranged along one axis. HRTEM image of the intermittent was displayed in the Figure.4B, and the magnified TEM image demonstrated the intermittent structure more clearly (S_Figure 3). From this image, it can be seen that the lattice directions of the yellow circles were obviously not along one same axes, this further indicated that the Ag-In-Zn-S intermittent nanorods were grown by several small Ag-In-Zn-S nanoparticles. Figure 4C is the TEM result of the as-obtained Ag-In-Zn-S nanorods reaction for half and two hrs, it can be seen that the as-synthesized Ag-In-Zn-S nanorods were ~2.4 nm in width and ~36 nm in length. In addition, it was clearly shown that nearly all the nanorods were curving, which was different with the intermittent rods shape. High resolution TEM image of curving Ag-In-Zn-S nanorods was showed in the Figure 4D, it could be observed that the rod structures were not straight. From the HRTEM of curving Ag-In-Zn-S nanorods, the lattice spacing was measured to be 0.29 nm which could be referenced to the (101) planes of hexagonal Ag-In-Zn-S structure.

After reaction for 3 hrs, a mixture of Ag-In-Zn-S straight and curving nanorods were achieved. Figure 5A shows the TEM image of the mixture of Ag-In-Zn-S straight and curving nanorods. It was observed that many of the straight Ag-In-Zn-S nanorods (labeled red rectangle) were evolved from the curving rod (labeled yellow circles) as the reaction time increased. Figure 5B shows a high magnification TEM image, which

clearly showed a mixture of straight and curving Ag-In-Zn-S nanorods. However; the curving Ag-In-Zn-S rods structure were taking up the majority. Therefore, after reaction for 4 hrs, nearly all the Ag-In-Zn-S nanorods became straight (Figure 2A).

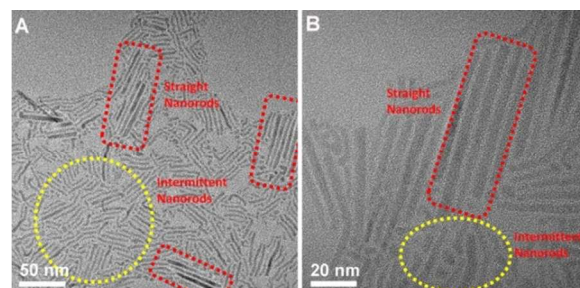


Figure 5. (A) TEM images of the Ag-In-Zn-S straight and curving nanorods mixture (B) Higher magnified TEM image of Ag-In-Zn-S straight and curving nanorods mixture.

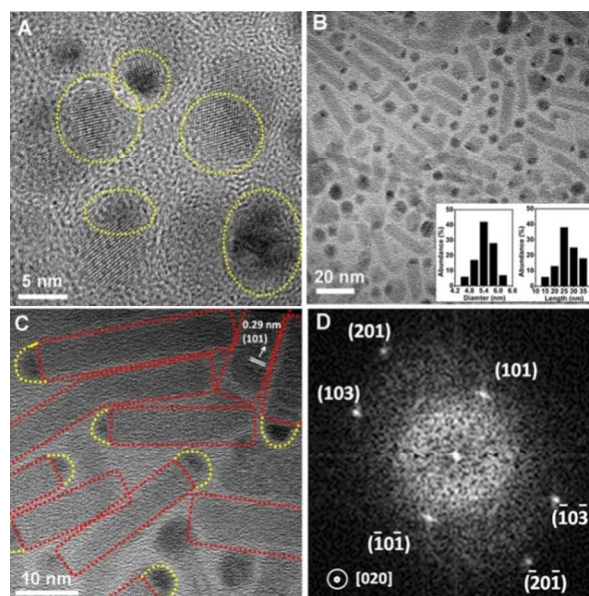


Figure 6. (A) TEM images of the Ag-In-Zn-S dimer nanoparticles (B) TEM images of the Ag-In-Zn-S dimer nanorods (inset: histograms showing the diameter and length distribution of the nanorods) (C) HRTEM image of several typical dimer nanorods, (D) is the 2D-FFT image of the as-synthesized Ag-In-Zn-S dimer nanorods.

In our reported results, we used hot injection to obtain AgInS₂-ZnS heterodimers with tunable photoluminescence²⁷⁻³⁰. Here, we changed some precursors and obtained unique nanorods with one part being Ag-In-Zn-S and the other part having higher silver composition. The TEM results and 2D-FFT images were showed in Figure 6, it can be seen that nearly all the dimer structures have a darker tip, which could be attributed to silver (Figure 6B). However; it was difficult to verify the exact composition of such a small part. From the lattice distance and 2D-FFT images of the as-prepared dimer structure, it could be one part of it is (101) planes of Ag-In-Zn-S, which is similar with the Ag-In-Zn-S straight nanorods. Regarding the other part, the Ag ions could easily form a complex with the surfactant, and the decomposition temperature would be

decreased^{34, 35}. This results in the Ag complex decomposing first to form as dimer structure. When the ultrasonic time was increased to 2 hrs, the dimer structure became shorter, which could be seen in Figure.6A.

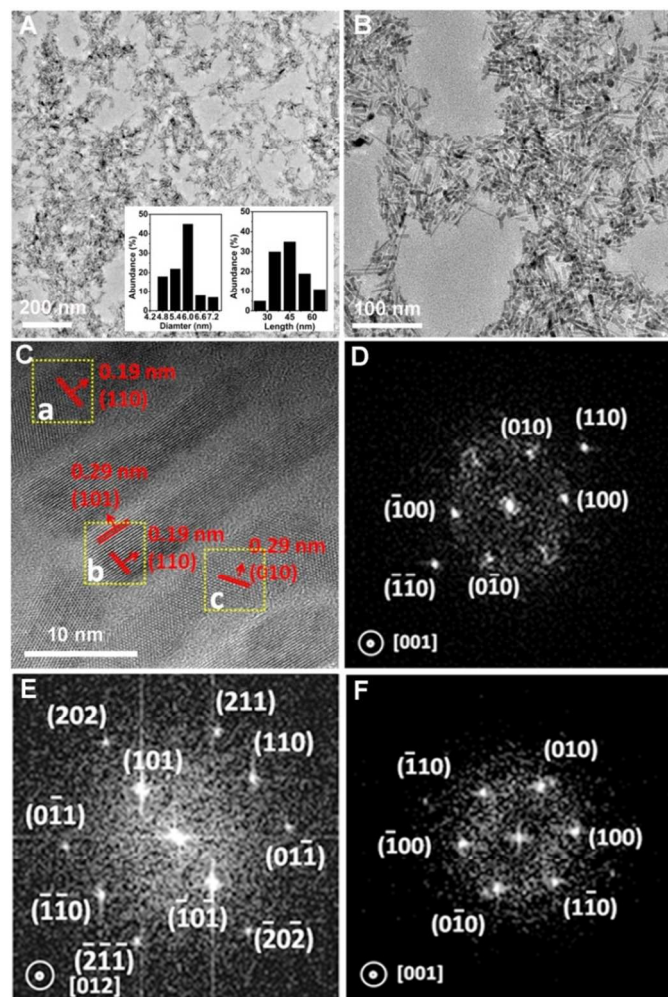
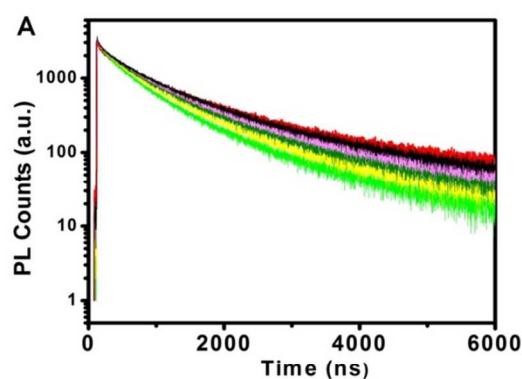


Figure 7. (A)TEM images of the Ag-In-Zn-S nail-like nanorods (inset: histograms showing the diameter and length distribution of the nanorods) (B) HRTEM image of several typical nail-like nanorods, (C), (D) and (E) are the 2D-FFT images of the as-synthesized nail-like nanorods of the different areas of Figure 7C labeled (a), (b) and (c) respectively.

Nail-like nanorods were synthesized using drop-injection method. In order to further investigate the detailed structure of the nail-like Ag-In-Zn-S nanorods obtained by drop-injection method, TEM was employed to observe the samples. Figure 7A shows the corresponding TEM images of the Ag-In-Zn-S nail-like nanorods. It could be seen that nearly all the obtained nanorods looked like nails, with a thick end and a narrower sharp end. Therefore we defined these nanorods as “nail-like”. Furthermore, the nail-like Ag-In-Zn-S nanorods could be well-dispersed, implying high nanocrystal quality. For confirming the elements composition of the Ag-In-Zn-S nail-like nanorods, energy dispersive X-ray spectroscopy was used for testing. As shown in S_Figure 4, four signals from silver, indium, zinc and sulphur elements were found in the spectrum, which demonstrated the sample was comprised of Ag, In, Zn and S. Moreover; the X-ray photoelectron spectroscopy (XPS) of the

as-prepared Ag-In-Zn-S nail-like nanorods was shown in S_Figure 5, which is consistent with the EDX results. The as-prepared Ag-In-Zn-S nanorods had diameter of about ~6.0 nm and length of ~45 nm, which could be further observed by the higher resolution TEM (Figure 7B). Figure 7C shows a typical HRTEM image of the nail-like Ag-In-Zn-S nanorod, and the two-dimensional fast Fourier transform (2D-FFT) of the relevant images were introduced (Figure 7 D, E and F). As shown in Figure 2C, the distance between two adjacent planes in the labeled “a” was measured to be 0.19 nm, corresponding to the (110) planes of hexagonal close-packed structure, which was also consistent with the results obtained from XRD patterns (S_Figure 6). The corresponding FFT image of the nanorods labeled “a” indicated that the [110] direction was aligned with the nanorod axis. Furthermore, the part labeled “b” in Figure 2C were measured to 0.19 nm and 0.29 nm, which corresponded to the (110) and (101) planes. The FFT image of part “b” of Figure 7C was shown in Figure 7E, which further confirmed the preferential growth along the [110] direction. Figure 3F shows the FFT image of part “c” in Figure 7C, which display the (010) planes.

The key of this synthetic method was the drop by drop addition of the zinc and sulfur precursors, which was probably the main reason for the formation of nail-like Ag-In-Zn-S nanorods. From our results reported before, the radius of zinc ion was nearly the same as indium and so silver ion could diffuse into the AgInS₂ nanoparticles at an elevated temperature. In our drop by drop in turn method, the zinc and sulfur precursors was added more slowly, which was much different with one time injection method. This was because the zinc and sulfur will be formed at some specific positions of the AgInS₂ nanoparticles and lead to the formation of nail-like nanorods. Similar results also reported Ag₂S and Cu₂S could be used as catalyst in the growth of AgInZn₇S₉ nanowires¹⁷. Therefore, the drop by drop method might be the reason for the growth of nail-like nanorods.



Wavelength (nm)	τ_1 /ns	A1/%	τ_2 /ns	A2/%
560	206	49.5	853	50.1
580	231	46.8	948	53.2
600	240	47.8	1035	52.2
620	267	48.8	1137	51.2
640	272	47.2	1218	52.8
660	280	47.4	1248	52.6

Figure 8. (A) PL relaxations of the Ag-In-Zn-S straight nanorods and (B) Table showing the fit parameters of the relaxation plots. The fit parameters are derived from the equation: $I(t) = A_1 \exp(-t/\tau_1) + A_2 \exp(-t/\tau_2)$.

In order to further study the effect of Ag-In-Zn-S nanorods PL behaviors of the nanocrystals, PL relaxations of the Ag-In-Zn-S straight nanorods were chosen for characterization, as shown in Figure 8A. Figure 8A showed the representative PL decay curves for straight Ag-In-Zn-S nanorods (emission at 620 nm), which were probed at different emissions wavelengths. In general, the PL relaxations of the samples were not single-exponential. After fitting the relaxation plot using the biexponential equation $I(t) = A_1 \exp(-t/\tau_1) + A_2 \exp(-t/\tau_2)$, the PL relaxations could be separated into two decay components^{18, 35-39}. Where τ_1 and τ_2 represent the decay time of the PL emission; A_1 and A_2 represent the amplitude of the decay components. From Figure 8B, it could be seen the lifetime of the straight Ag-In-Zn-S nanorods displayed long lifetime achieved to 1.248 μ s, which was completely different from the previously reported results³⁵⁻³⁹.

Usually, in binary semiconductor nanoparticles, electrons and holes combine quickly and the PL lifetimes are only tens of nanoseconds due to the direct band gap and surface states. In the Ag-In-Zn-S nanorods, excitons easily formed intrinsic point defects due to the existence of three kinds of different sized cations. Due to the large number of intrinsic defects, the Ag-In-Zn-S rod structure determines the ratio of the radiative recombination from surface and intrinsic states, which are lower than nanoparticles³⁵⁻³⁹. Therefore, the lifetime of the straight Ag-In-Zn-S nanorods has a significantly longer lifetime. In this sense, the time-resolved measurements indicated that there exist two PL radiative mechanisms in the nanorods and the PL decay time increasing with the PL wavelength. The long-lived excitons of the straight Ag-In-Zn-S nanorods may provide potential applications as photocatalysts and photovoltaic³⁸.

Conclusions

In summary, we have developed a facile approach to synthesize Ag-In-Zn-S straight nanorods with \sim 5 nm in width and \sim 100 nm in length. Furthermore, the detailed growth mechanism of the Ag-In-Zn-S straight nanorods was discussed. Furthermore; the photoluminescence of the Ag-In-Zn-S straight nanorods could be tuned from 550 nm to 650 nm by adjusting the composition of the rods. And the as-prepared Ag-In-Zn-S straight nanorods demonstrated a long lifetime achieved to 1.248 μ s, which may provide potential applications in photocatalysis and photovoltaics. On the other hand, nail-like Ag-In-Zn-S nanorods and rod-particle dimer structures were achieved by adjusting reaction parameters, and the emissions of the nanorods nail-like Ag-In-Zn-S nanorods and rod-particle dimer structures could be tuned by the composition.

Acknowledgements

This work is supported by the initial funding of Hundred Young Talents Plan at Chongqing University (No. 0210001104430 and No. 0210001104431).

Notes and references

^aKey Laboratory of Optoelectronic Technology and Systems of the Education Ministry of China, College of Optoelectronic Engineering, Chongqing University, Chongqing 400044, China
E-mail: xstang@cqu.edu.cn

^bCollege of Chemistry and Chemical Engineering, Chongqing University, Chongqing 400044, China

^cDepartment of Materials Science & Engineering, Faculty of Engineering, National University of Singapore, Singapore

Electronic Supplementary Information (ESI) available: supplementary figures (EDS, XRD, TEM). See DOI: 10.1039/b000000x/

- 1 V. L. Colvin, M. C. Schlamp, A. P. Alivisatos, *Nature* 1994, **370**, 354.
- 2 S. Coe, W. K. Woo, M. G. Bawendi, V. Bulovic, *Nature* 2002, **420**, 800.
- 3 N. Tessler, V. Medvedev, M. Kazes, S. Kan, U. Banin, *Science* 2002, **295**, 1506.
- 4 J. Zhang, R. Xie, W. Yang, *Chem. Mater.* 2011, **23**, 3357.
- 5 P. Brown, P. V. Kamat, *J. Am. Chem. Soc.* 2008, **130**, 8890.
- 6 M. Bruchez, M. Moronne, P. Gin, S. Weiss, A. P. Alivisatos, *Science*, 1998, **282**, 2013.
- 7 W. C. W. Chan, S. M. Nie, *Science* 1998, **281**, 2016.
- 8 J. Z. Wang, M. Lin, Y. Yan, Z. Wang, P. C. Ho, K. P. Loh, *J. Am. Chem. Soc.*, 2009, **131**, 11300.
- 9 C. Kirchner, T. Liedl, K. Stefan, T. Pellegrino, A. M. Javier, H. E. Gaub, S. Stölzle, N. Fertig, W. J. Parak, *Nano Lett.* 2005, **5**, 331.
- 10 S. Deka, A. Quarta, M. G. Lupo, A. Falqui, S. Boninelli, C. Giannini, G. Morello, M. D. Giorgi, G. Lanzani, C. Spinella, R. Cingolani, T. Pellegrino, L. Manna *J. Am. Chem. Soc.*, 2009, **131**, 2948.
- 11 C. B. Murray, D. J. Norris, M. G. Bawendi, *J. Am. Chem. Soc.*, 1993, **115**, 8706.
- 12 W. W. Yu, X. G. Peng, *Angew. Chem. Int. Ed.*, 2002, **41**, 2368
- 13 R. Xie, J. Zhang, F. Zhao, W. Yang, X. Peng, *Chem. Mater.*, 2010, **22**, 3820.
- 14 R. Xie, M. Rutherford, X. Peng, *J. Am. Chem. Soc.*, 2009, **131**, 5691
- 15 H. Borchert, D. Dorfs, C. McGinley, S. Adam, T. Möller, H. Weller, A. Eychmüller *J. Phys. Chem. B*, 2003, **107**, 7486
- 16 T. Torimoto, T. Adachi, K. Okazaki, M. Sakuraoka, T. Shibayama, B. Ohtani, A. Kudo, S. Kuwabata, *J. Am. Chem. Soc.*, 2007, **129**, 12388
- 17 C. Zou, M. Li, L. Zhang, Y. Yang, Q. Li, X. Chen, X. Xu, S. Huang, *Cryst. Eng. Comm.*, 2011, **13**, 3515
- 18 S. P. Hong, H. K. Park, J. H. Oh, H. Yang, Y. R. Do, *J. Mater. Chem.*, 2012, **22**, 18939
- 19 K. Kadlag, P. Patil, M. Rao, S. Datta, A. Nag, *Cryst. Eng. Comm.*, 2014, **16**, 4410
- 20 S. J. Lee, Y. Kim, J. Jung, M. A. Kim, N. Kim, S. J. Lee, S. K. Kim, Y. Kim, J. K. Park, *J. Mater. Chem.*, 2012, **22**, 11957
- 21 W. Chung, H. Jung, C. Lee, S. Kim, *J. Mater. Chem. C*, 2014, **2**, 4227
- 22 X. Yang, Y. Tang, S. T. Tan, M. Bosman, Z. Dong, K. S. Leck, Y. Ji, H. V. Demir, X. W. Sun, *Small*, 2013, **9**, 2689
- 23 W. Zhang, X. Zhong, *Inorg. Chem.*, 2011, **50**, 4065
- 24 L. Yi, Y. Liu, N. Yang, Z. Tang, H. Zhao, G. Ma, Z. Su, D. Wang, *Energy Environ. Sci.*, 2013, **6**, 835
- 25 Q. Liu, Z. Zhao, Y. Lin, P. Guo, S. Li, D. Pan, X. Ji, *Chem. Commun.*, 2011, **47**, 964
- 26 F. Huang, J. Zhou, J. Xu, Y. Wang, *Nanoscale*, 2014, **6**, 2340
- 27 B. Koo, R. N. Patel, B. A. Korgel, *J. Am. Chem. Soc.*, 2009, **131**, 3134
- 28 Y. A. Wang, X. Zhang, N. Bao, B. Lin, A. Gupta, *J. Am. Chem. Soc.*, 2011, **133**, 11072
- 29 X. Tang, W. Cheng, E. S. G. Choo, J. Xue *Chem. Commun.*, 2011, **47**, 5217
- 30 X. Tang, W. Ho, J. Xue, *J. Phys. Chem. C*, 2012, **116**, 9769
- 31 X. G. Peng, L. Manna, W. D. Yang, J. Wickham, E. Scher, A. Kadavanich, A. P. Alivisatos, *Nature*, 2000, **404**, 59

- 32 J. Wang, M. S. Gudiksen, X. Duan, Y. Cui, C. M. Lieber, *Science*, 2001, **293**, 1455
- 33 J. Hu, L. S. Li, W. Yang, L. Manna, L.W. Wang, A. P. Alivisatos, *Science*, 2001, **292**, 2060
- 34 H. Zhong, S. S. Lo, T. Mirkovic, Y. Li, Y. Ding, Y. Li, G. D. Scholes, *ACS Nano*, 2010, **9**, 5253
- 35 H. Zhong, Y. Zhou, M. Ye, Y. He, J. Ye, C. He, C. Yang, Y. Li, *Chem. Mater.*, 2008, **20**, 6434
- 36 L. Li, A. Pandey, D. Werder, B. Khanal, J. Pietryga, V. Klimov, *J. Am. Chem. Soc.*, 2011, **133**, 1176
- 37 B. B. Srivastava, S. Jana, N. Pradhan, *J. Am. Chem. Soc.*, 2011, **133**, 1007
- 38 B. Mao, C. Chuang, J. Wang, C. Burda, *J. Phys. Chem. C*, 2011, **115**, 8945
- 39 Y. Hamanaka, T. Ogawa, M. Tsuzuki, *J. Phys. Chem. C*, 2011, **115**, 1786